JOURNAL OF MATERIALS SCIENCE, 32 (1997) 2341–2346

Stochastic analysis on crack path of polycrystalline ceramics based on the difference between the released energies in crack propagation

J. TATAMI*, K. YASUDA, Y. MATSUO
Department of Inorganic Materials, Faculty of Engineering, Tokyo Institute of Technology, Tokyo, Japan

S. KIMURA
Institute of Inorganic Synthesis, Faculty of Engineering, Yamanashi University, Japan

The crack path of polycrystalline ceramics has been theoretically analysed with a stochastic model based on the difference between the released energies in intergranular and transgranular crack propagation. Assuming that the path with the lowest released energy should be realized as the actual crack path, the expected values of the fraction of transgranular fracture on fracture surface and the fracture toughness of polycrystalline ceramics were formulated as functions of grain size and the critical energy release rates of grain and grain boundary. By comparison between the theory and the experimental results it was shown that the stochastic model proposed here expressed the change of the crack path and the fracture toughness of polycrystalline Al_2O_3, relative to grain size.

1. Introduction

In order to improve the fracture toughness of ceramics, many studies have been conducted on whisker reinforcement [1–3], particle dispersion [4–6] and microstructural control [7–15]. However, it is now necessary to investigate the relationship between the microstructure (grain size, pores and inclusions) and the fracture toughness of ceramics, because even the relationship for single phase ceramics has not yet been fully understood. Aiming at this point, the authors in the previous report [15] measured fracture toughness of polycrystalline Al_2O_3 with different grain sizes by controlled surface flaw (CSF) method and chevron notched beam (CN) method. As a result, it was found that the fracture toughness K_{IC} of polycrystalline Al_2O_3 is approximately 3.8 $MPa\,m^{1/2}$ with a grain size of 1.8 μm, increases with an increase in grain size, and becomes constant at approximately 4.5 $MPa\,m^{1/2}$ with grain sizes more than 30 μm. Furthermore, it was revealed that the critical energy release rate calculated from K_{IC} linearly increases with an increase in the fraction of transgranular fracture on fracture surface (hereafter the fraction of transgranular fracture).

Based on this result, the authors analysed the influence of grain size on the fraction of transgranular fracture of polycrystalline ceramics from perspectives in the previous study [16]. It is assumed that the fracture of polycrystalline ceramics is a probability even such that a crack propagates in the microstructure, which consists of crystal grains in random orientation. Therefore, the fraction of transgranular fracture obtained as a result of crack propagation is also expressed as the expected value of the probability event. Our previous stochastic model [16] was roughly able to explain the influence of grain size on the fraction of transgranular fracture in polycrystalline Al_2O_3. However, the parameters for selective probability of crack path had to be assumed in the previous theory so that theory was not a physical model based on energy dissipation during crack extension.

In this paper, assuming that the path with the lowest released energy is realized as the actual crack path, comparison between the released energies in transgranular or intergranular crack propagation leads to the selective probability of crack path theoretically. In addition, the modified stochastic model proposed in this paper is compared with the experimental results [15] in order to discuss the validity of the analysis.

2. Theory

2.1. Two-dimensional polycrystal with square grains

In this analysis, as shown in Fig. 1, we assume a two-dimensional polycrystal (unit thickness) which consists of square grains with the critical energy release rate G_{IC}^{grain} and grain boundaries with the critical energy release rate $G_{IC}^{boundary}$. These critical energy release rates of grain and grain boundary are assumed to be constant as a first approximation. Here, the propagating direction of a main crack is denoted by x-direction, and the direction perpendicular to the main crack is

* Author to whom correspondence should be addressed.

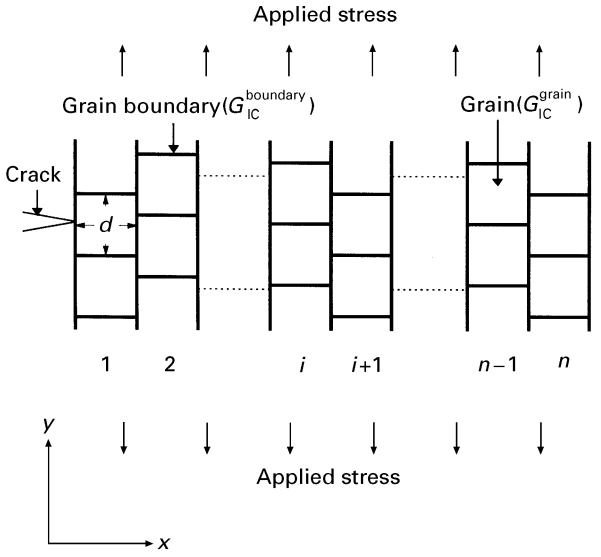

Figure 1 Schematic illustration of a microstructure model.

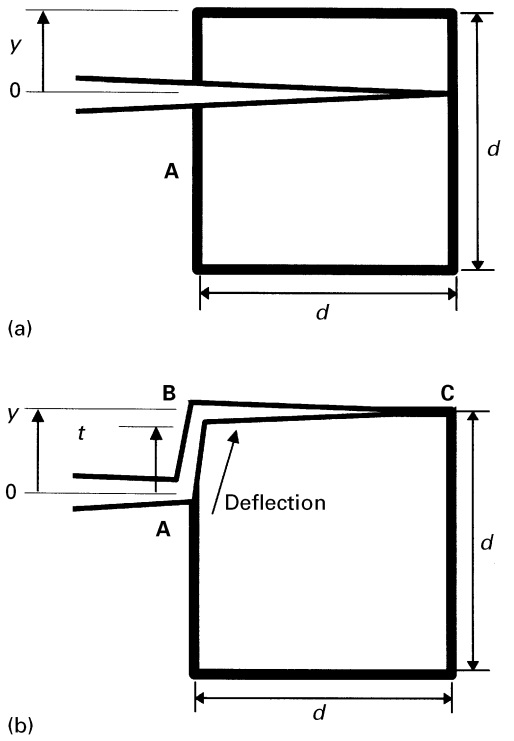

Figure 2 Schematic illustration of (a) transgranular crack propagation, (b) intergranular crack propagation.

denoted by y-direction. It is assumed that there is no correlation between locations in the y-direction of the i-th crystal grain and $(i + 1)$th crystal grain in the two-dimensional polycrystal, and that a crack extends at any locations of grain boundary in the y-direction with equal probability (Bernoulli trial [17]). It is also assumed that the main crack passes through n grains as it virtually propagates when uniaxial tensile stress is loaded in the y-direction.

During intergranular crack extension, the main crack propagates while deflecting 90° in this microstructure. Although the crack rarely deflects 90° in actual materials, the microstructure shown in Fig. 1 is adopted because the Bernoulli trial should be introduced in the new theory.

2.2. Released energy in crack propagation

In this paper, as shown in Fig. 2, we calculated the released energy in case that a crack propagates transgranularly or intergranularly after the crack arrived at the point **A** which is y distant from a grain boundary. Here y ranges from 0 to $d/2$ (d: grain size) to take symmetry into consideration. The released energy in transgranular fracture (W^{trans}) is estimated on the assumption that a crack coplanarly propagates in the grain as shown in Fig. 2a. Although the energy release rate of grain (G_{IC}^{grain}) is a function of the fracture toughness of cleavage planes and the angle between cleavage planes and a main crack (i.e. the selective angle of transgranular fracture in the previous paper [16]), it is assumed to be a constant value as an average in this paper. After the crack extends to the point **A**, the released energy in transgranular crack propagation can be expressed as follows

$$W^{trans} = \int_0^d G_{IC}^{grain}\,dx = G_{IC}^{grain}\,d \quad (1)$$

The released energy in intergranular fracture (W^{inter}) as shown in Fig. 2b is divided into two parts, namely, the crack deflection into y-direction and the crack propagation into x-direction. Therefore, the released energy is given by

$$W^{inter} = \int_0^y \tilde{G}_{IC}^{deflection}(t)\,dt + \int_0^d G_{IC}^{boundary}\,dx \quad (2)$$

where the first term in the right hand of Equation 2 corresponds to the dissipative energy during crack deflection from point **A** to **B** in Fig. 2b, and the second term to crack propagation from point **B** to **C**. Here, $\tilde{G}_{IC}^{deflection}(t)$ is the apparent critical energy release rate during crack deflection and t is deflected length. In order to estimate $\tilde{G}_{IC}^{deflection}(t)$, the following approach is used.

When a crack deflects from point **A** to **B**, the deflecting crack which has the main crack length ($2a$) under the tensile stress (σ), as shown in Fig. 3, is more difficult to propagate with longer deflected length (t). The stress intensity factor (K_I^B) at point **B** in Fig. 3 is expressed by the following equation [18]

$$K_I^B = F(t)\sigma a^{1/2} \quad (3)$$

where $F(t)$ is the shape factor dependent on crack geometry and deflected length (t), which was numerically calculated by Chatterjee using conformal mapping. The apparent stress intensity factor $\tilde{K}_I$ under the main crack length ($2a$) and the tensile stress (σ) is expressed as follows

$$\tilde{K}_I = \sigma(\pi a)^{1/2} \quad (4)$$

Assuming that a crack propagates when K_I^B reaches to the critical stress intensity factor of grain boundary ($K_{IC}^{boundary}$), the apparent fracture toughness ($\tilde{K}_{IC}^{deflection}(t)$) during crack deflection is expressed by

$$\tilde{K}_{IC}^{deflection}(t) = K_{IC}^{boundary}\frac{\pi^{1/2}}{F(t)} \quad (5)$$

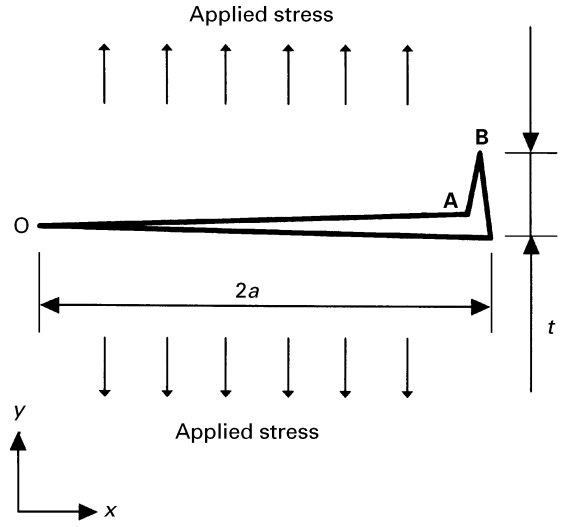

Figure 3 Schematic illustration of a deflected crack.

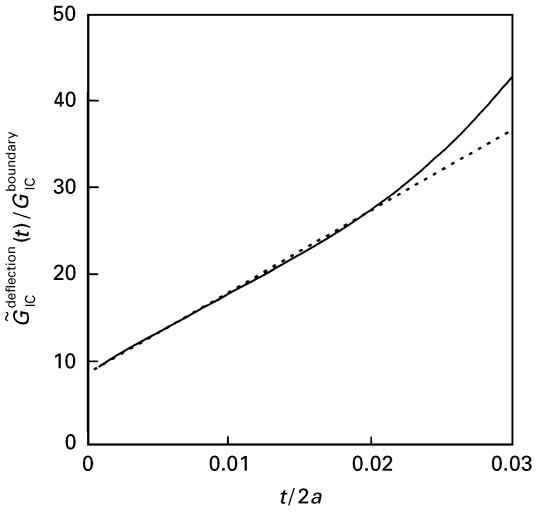

Figure 4 The relationship between normalized deflected length ($t/2a$) and normalized apparent critical energy release rate ($\tilde{G}_{IC}^{deflection}(t)/G_{IC}^{boundary}$). The solid line is a calculated curve by conformal mapping method [18]. The dotted line is a regression line.

Therefore, the apparent critical energy release rate ($\tilde{G}_{IC}^{deflection}(t)$) during crack deflection becomes as follows

$$\frac{\tilde{G}_{IC}^{deflection}(t)}{G_{IC}^{boundary}} = \frac{\pi}{F(t)^2} \tag{6}$$

The solid line in Fig. 4 shows the relationship between the normalized deflected length ($t/2a$) and the normalized apparent critical energy release rate ($\tilde{G}_{IC}^{deflection}(t)/G_{IC}^{boundary}$) in case of deflecting 90° [18]. This indicates that $\tilde{G}_{IC}^{deflection}(t)/G_{IC}^{boundary}$ is an incremental function of $t/2a$. Consequently, in the small region of $t/2a$ ($0 \leqslant t/2a \leqslant 0.02$), $\tilde{G}_{IC}^{deflection}(t)/G_{IC}^{boundary}$ is approximated by the following linear function

$$\frac{\tilde{G}_{IC}^{deflection}(t)}{G_{IC}^{boundary}} = p'\left(\frac{t}{2a}\right) + q = pt + q \tag{7}$$

The value of p' and q estimated by linear regression analysis using Equation 7 were 9.5×10^2 and 8.5, respectively. In the previous study, the fracture toughness was measured by the controlled surface flaw (CSF) method and the chevron notched beam (CN) method. The value of p is $0.32\ \mu m^{-1}$ for CSF specimens from calculation by the value of p' and the actual crack lengths a ($= 150\ \mu m$) and the value of p is $3.2\ \mu m^{-1}$ for CN specimens from calculation by the value of p' and the actual crack length a ($= 1.5$ mm). By substituting Equation 7 into Equation 2, therefore, the released energy in a crack propagation from point **A** to **B** in Fig. 2b is equal to

$$\int_0^y G_{IC}^{deflection}(t)\,dt = G_{IC}^{boundary}\left(\frac{1}{2}py^2 + qy\right) \tag{8}$$

It is assumed that the critical energy release rate for propagating from point **B** to **C** in Fig. 2b is equal to $G_{IC}^{boundary}$, namely

$$\int_0^d G_{IC}^{boundary}\,dx = G_{IC}^{boundary}\,d \tag{9}$$

Therefore, by substituting Equations 9 and 8 into Equation 2, the released energy in intergranular fracture is approximately equal to

$$W^{inter} = G_{IC}^{boundary}\left(d + \frac{1}{2}py^2 + qy\right) \tag{10}$$

As shown in Equations 1 and 10, the released energy in transgranular or intergranular crack propagation was formulated as a function of grain size (d).

2.3. Determination of the crack path

It is assumed that the path with the lowest released energy is realized as the actual crack path, that is, the crack path is determined using the following equation

$$\begin{aligned}\Delta W &= W^{trans} - W^{inter} \\ &= G_{IC}^{grain}\,d \\ &\quad - G_{IC}^{boundary}\left(d + \frac{1}{2}py^2 + qy\right)\end{aligned} \tag{11}$$

If ΔW is a positive number, the crack propagates intergranularly because the released energy in intergranular crack propagation is lower than transgranular crack propagation. Thus, depending on sign of the released energy in crack propagation (ΔW), the actual crack path is determined as follows

$$\begin{cases} \Delta W > 0 & \text{(a crack propagates intergranularly)} \quad 0 \leqslant y < y_C \\ \Delta W \leqslant 0 & \text{(a crack propagates transgranularly)} \quad y_C \leqslant y \leqslant \dfrac{1}{2}d \end{cases} \tag{12}$$

In other words, as shown in Fig. 5, an assumption is made that when a crack arrives within the selective region of intergranular fracture with a length of y_C (which was supposed to be a constant value *a priori* in the previous study [16]), the crack propagates intergranularly. y_C is defined by the condition

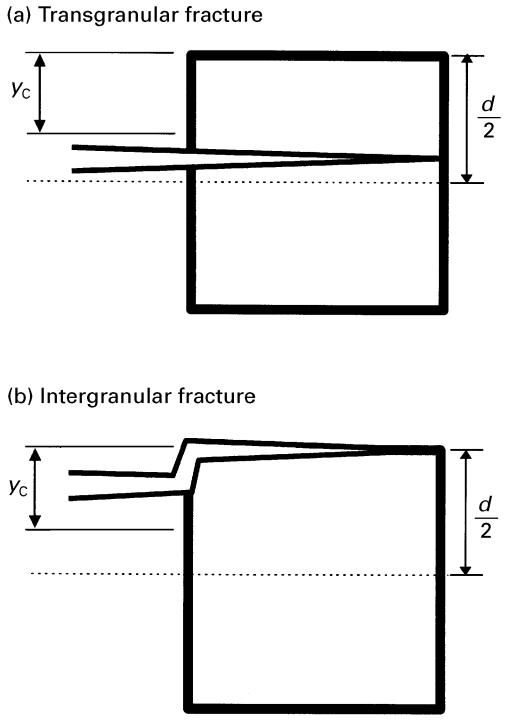

Figure 5 The relationship between crack path and arrival position of a crack.

$\Delta W = 0$. Therefore

$$-\frac{1}{2}\,G_{IC}^{boundary} p y_C^2 - G_{IC}^{boundary} q y_C + (G_{IC}^{grain} - G_{IC}^{boundary}) d = 0 \tag{13}$$

As a result, y_C is derived as a function of grain size (d) and the ratio of the critical energy release rate of grain to that of grain boundary, ($G_{IC}^{grain}/G_{IC}^{boundary}$) as follows

$$y_C = \frac{-q + \left[q^2 + 2\left(\frac{G_{IC}^{grain}}{G_{IC}^{boundary}} - 1\right) pd\right]^{1/2}}{p} \quad (d \geqslant d^*)$$

$$y_C = \frac{d}{2} \quad (0 < d < d^*) \tag{14}$$

Taking it into consideration that y_C ranges from 0 to $d/2$ (d: grain size), as same as y, y_C is classified according to grain size. Here, d^* in Equation 14 is expressed as follows

$$d^* = \frac{8\left(\frac{G_{IC}^{grain}}{G_{IC}^{boundary}} - 1\right) - 4q}{p} \tag{15}$$

Consequently, the crack path after reaching the point **A** of the grain boundary is determined using Equations 12 and 14.

2.4. Derivation of the fraction of transgranular fracture and the critical energy release rate

First, the fraction of transgranular fracture is derived. As a result of above section, the probability which a crack propagates transgranularly and intergranularly is expressed as follows

$$y_C \Big/ \left(\frac{d}{2}\right) = \frac{2y_C}{d} \quad \text{(intergranular fracture)}$$

$$1 - y_C \Big/ \left(\frac{d}{2}\right) = \frac{d - 2y_C}{d} \quad \text{(transgranular fracture)} \tag{16}$$

Assuming that a crack virtually propagates through n grains and that k grains break transgranularly, which leads to the fraction of transgranular fracture to be k/n. Thus, based on Equation 16, the expected value of the fraction of transgranular fracture ($\hat{f}$) becomes

$$\hat{f} = \sum_{k=0}^{n} \frac{k}{n}\,{}_nC_k \left(\frac{d - 2y_C}{d}\right)^k \left(\frac{2y_C}{d}\right)^{n-k} \tag{17}$$

Equation 17 is arranged using the binomial theorem, as follows

$$\hat{f} = \frac{d - 2y_C}{d} \sum_{k=1}^{n} {}_{n-1}C_{k-1} \left(\frac{d - 2y_C}{d}\right)^{k-1} \left(\frac{2y_C}{d}\right)^{n-k} = \frac{d - 2y_C}{d} \tag{18}$$

Thus, taking it into consideration that y_C is a function of grain size (d) and the ratio of the critical energy release rate of grain to that of grain boundary ($G_{IC}^{grain}/G_{IC}^{boundary}$), the expected value of the fraction of transgranular fracture ($\hat{f}$) is also a function of d and $G_{IC}^{grain}/G_{IC}^{boundary}$.

Next, the critical energy release rate is derived. When assuming that the crack virtually propagates in x-direction by a distance ($L = nd$) which is assumed to be sufficiently shorter than the length of a main crack ($2a$), using Equations 1 and 10, the expected value of the released energy ($\hat{\Gamma}$) of an actual crack extension can be expressed as follows

$$\hat{\Gamma} = G_{IC}^{grain} \hat{f} L + G_{IC}^{boundary} \left[1 + \frac{1}{dy_C} \int_0^{y_C} \left(\frac{1}{2}\,py^2 + qy\right) \mathrm{d}t\right] \times (1 - \hat{f}) L \tag{19}$$

Therefore, based on Equations 17 and 19, the expected value of the critical energy release rate ($\hat{G}_{IC}$) is expressed by

$$\begin{aligned}\hat{G}_{IC} &\equiv \frac{\hat{\Gamma}}{L} \\ &= G_{IC}^{grain} \hat{f} + G_{IC}^{boundary} \left[1 + \frac{1}{dy_C} \int_0^{y_C} \left(\frac{1}{2}\,py^2 + qy\right) \mathrm{d}y\right] (1 - \hat{f}) \\ &= G_{IC}^{grain} \left(1 - \frac{2y_C}{d}\right) + G_{IC}^{boundary} \left(1 + \frac{p}{6d}\,y_C^2 + \frac{q}{2d}\,y_C\right) \frac{2y_C}{d}\end{aligned} \tag{20}$$

Thus, the critical energy release rate was a function of grain size, (d) and the critical energy release rate of grain and grain boundary (G_{IC}^{grain} and $G_{IC}^{boundary}$).

3. Discussion

3.1. Influence of grain size on the fraction of transgranular fracture and the critical energy release rate

Fig. 6 shows an example of the numerical calculations of the theory on the fraction of transgranular fracture (Equation 18) taking p as $2\ \mu m^{-1}$, q as 8.5, G_{IC}^{grain} as $50\ J\,m^{-2}$ where G_{IC}^{grain} is calculated taking the fracture toughness as $4\ MPa\,m^{1/2}$, Young's modulus as 300 GPa and Poisson's ratio as 0.25. The solid lines designate changes in the expected value of the fraction of transgranular fracture accompanying a change in grain size when $G_{IC}^{boundary}$ varied from $2\ J\,m^{-2}$, which is typical value of thermodynamic surface energy of ceramics [19], to $50\ J\,m^{-2}$, which is equal to G_{IC}^{grain}. This indicates that the fraction of transgranular fracture increases with an increase in grain size. Furthermore, it is found that the expected value of the transgranular fracture $\hat{f}$ increases with an increase in $G_{IC}^{boundary}$ and it reaches a constant value ($\hat{f} = 1$) $G_{IC}^{boundary}$ is equal to G_{IC}^{grain}.

Fig. 7 shows an example of the numerical calculation of the theory on the critical energy release rate (Equation 20). The solid lines designate changes in the expected value of the critical energy release rate accompanying a change in grain size when $G_{IC}^{boundary}$ was varied between $2\ J\,m^{-2}$ and $50\ J\,m^{-2}$ taking p as $2\ \mu m^{-1}$, q as 8.5, G_{IC}^{grain} as $50\ J\,m^{-2}$. This indicates that the critical energy release rate increases with an increase in grain size. Furthermore, it is found that the expected value of the critical energy release rate $\hat{G}_{IC}$ increases with an increase in $G_{IC}^{boundary}$ and it reaches a constant value ($\hat{G}_{IC} = G_{IC}^{grain}$) when $G_{IC}^{boundary}$ is equal to G_{IC}^{grain}.

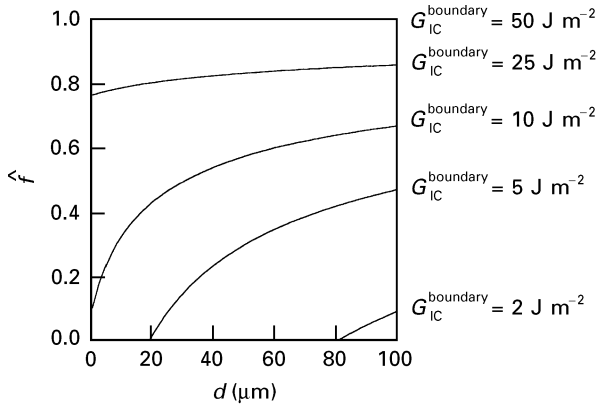

Figure 6 The influence of $G_{IC}^{boundary}$ on the fraction of transgranular fracture estimated by Equation 17.

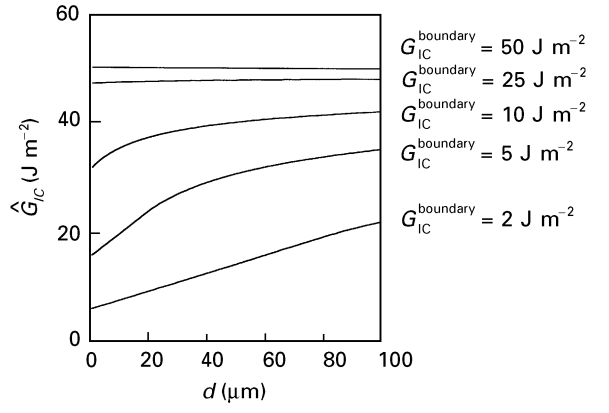

Figure 7 The influence of $G_{IC}^{boundary}$ on the critical energy release rate estimated by Equation 20.

3.2. Comparison between theory and experimental results

In the previous paper [15], the fracture toughness and the fraction of transgranular fracture of polycrystalline Al_2O_3 were measured using the controlled surface flaw (CSF) method and the chevron notched beam (CN) method. In this paper, the fraction of transgranular fracture and the critical energy release rate are derived as a function of grain size (d) and the critical energy release rate of grain and grain boundary. Therefore, the theory is compared with the experimental results in the previous paper [15].

3.2.1. Comparison between theory and experimental results on the fraction of transgranular fracture

Here, the theory on the fraction of transgranular fracture (Equation 18) is compared with the experimental results in the previous paper [15]. Fig. 8 shows the experimental data of the CSF specimens (open circles in Figs 8 and 9) and of the CN method (closed circles in Figs 8 and 9) on the fraction of transgranular fracture and the regression curves which were estimated by a least squares method using Equation 18 and experimental data [15]. In the least squares method, by changing $G_{IC}^{grain}/G_{IC}^{boundary}$, we tried to make both curves of the CSF method and the CN method most suitable for each experimental result at the same time. Here, q was set to 8.5, and p to $3.2\ \mu m^{-1}$ for the CSF specimens (crack length a of CSF specimens is 150 μm) and to $0.32\ \mu m^{-1}$ for the CN specimens (crack length a of CSF specimens is 150 μm). This figure indicates that both the theoretical curves monotonically increase with an increase in grain size, and

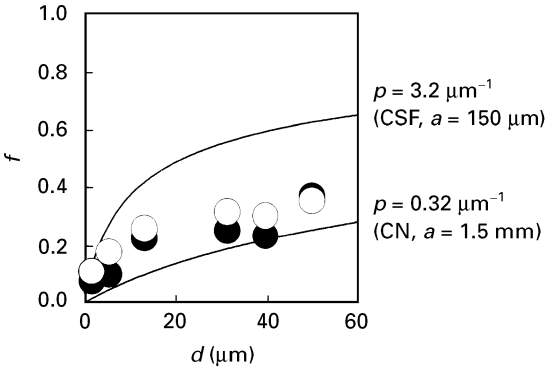

Figure 8 The relationship between grain size and the fraction of transgranular fracture. Open circles indicate experimental data on CSF specimens. Closed circles indicate experimental data on CN specimens. Parameters for drawing solid lines are $G_{IC}^{grain}/G_{IC}^{boundary} = 5.3$, $q = 8.5$, $p = 0.32\ \mu m^{-1}$, $3.2\ \mu m^{-1}$.

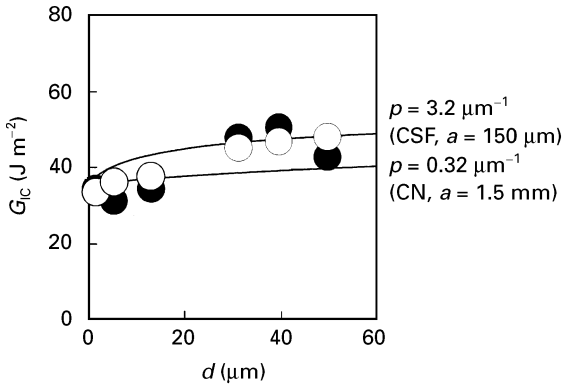

Figure 9 The relationship between grain size and the critical energy release rate. Open circles indicate experimental data on CSF specimens. Closed circles indicate experimental data on CN specimens. Parameters for drawing solid lines are $G_{IC}^{grain} = 59\ J\,m^{-2}$, $G_{IC}^{boundary} = 11\ J\,m^{-2}$, $q = 8.5$, $p = 0.32\ \mu m^{-1}$, $3.2\ \mu m^{-1}$.

they express the tendency of the grain size dependence on the fraction of transgranular fracture of polycrystalline Al_2O_3. Furthermore, the value of the ratio of the critical energy release rate of grain to that of grain boundary ($G_{IC}^{grain}/G_{IC}^{boundary}$) estimated by the regression analysis is 5.2.

It may be strange that this theory is dependent on the main crack length, however, it can be understood by taking into consideration the fact that the crack deflection 90° cause the overestimation of p and q. If a deflected angle is smaller, p is not much dependent on the main crack length ($2a$) and this theoretical result for the CSF method agrees with CN method.

As stated above, it is revealed that the stochastic model proposed in this study expresses the change in the fraction of transgranular fracture, namely, the crack path.

3.2.2. Comparison between theory and experimental results on the critical energy release rate

Here, the theory on the critical energy release rate is compared with the experimental results in the previous paper [15]. Fig. 9 shows the experimental data of the CSF specimens (open circles in Figs 8 and 9) and of the CN method (closed circles in Figs 8 and 9) on the critical energy release rate and the regression curves which were estimated by a least squares method using Equation 20 and experimental data [15]. In the least squares method, by changing G_{IC}^{grain} and $G_{IC}^{boundary}$, we tried to make both curves of the CSF method and the CN method most suitable for each experimental result at the same time. Here, $G_{IC}^{grain}/G_{IC}^{boundary}$ was set to as 5.3, q to 8.5, and p to $3.2\ \mu m^{-1}$ for the CSF specimens and to $0.32\ \mu m^{-1}$ for the CN specimens. This figure indicates that both the theoretical curves monotonically increase with an increase in grain size, and they express the tendency of the grain size dependence on the critical energy release rate of polycrystalline Al_2O_3. Furthermore, the value of G_{IC}^{grain} and $G_{IC}^{boundary}$ estimated by the regression analysis were $59\ J\,m^{-2}$ and $11\ J\,m^{-2}$, respectively. Although detailsof these values have not been understood yet, it reveals that grain in polycrystalline Al_2O_3 is tougher than grain boundary. In the future, these values should be estimated by other ways, for example, measuring fracture toughness of single crystal and bicrystal.

As shown in the above, the stochastic model proposed here expresses the change in the critical energy release rate, that is, the fracture toughness relative to grain size.

4. Conclusions

The crack path of polycrystalline ceramics has been theoretically analysed with a stochastic model based on the difference between the released energies in intergranular and transgranular crack propagation. Assuming that the path with the lowest released energy should be realized as the actual crack path, the expected values of the fraction of transgranular fracture on fracture surface and the fracture toughness of polycrystalline ceramics were formulated as functions of grain size and the critical energy release rates of grain and grain boundary. By comparison between the theory and the experimental results, it was shown that the stochastic model proposed here expressed the change of the crack path and the fracture toughness of polycrystalline Al_2O_3 relative to grain size.

References

1. N. CLAUSSEN, K. L. WEISSKOPH and M. RÜHLE, *J. Amer. Ceram. Soc.* **69** (1986) 288.
2. E. YASUDA, T. AKATSU, Y. TANABE, *J. Ceram. Soc. Japan* **99** (1991) 52.
3. P. F. BECKER, E. R. FULLER, Jr. and P. ANGELINI, *J. Amer. Ceram. Soc.* **74** (1991) 2131.
4. D. P. H. HASSELMAN and R. M. FULRATH, *ibid.* **49** (1966) 68.
5. F. F. LANGE, *ibid.* **57** (1971) 614.
6. A. NAKAHIRA, K. NIIHARA and T. HIRAI, *J. Ceram. Soc. Japan* **94** (1986) 767.
7. N. CLAUSSEN, R. PABST and C. P. LAHMANN, *Proc. Brit. Ceram. Soc.* **25** (1975) 139.
8. P. L. PLATT, "Fracture", edited by D. M. R. Tappin (University of Waterloo, Waterloo Press, 1977) p. 909.
9. B. MUSSLER, M. V. SWAIN and M. CLAUSSEN, *J. Amer. Ceram. Soc.* **65** (1982) 566.
10. K. HAYASHI, K. GOTO and T. NISHIDA, *J. Ceram. Soc. Japan* **99** (1991) 620.
11. T. NISHIDA and I. KAMEYAMA, *ibid.* **100** (1992) 276.
12. M. SAKAI, R. C. BRADT and A. S. KOBAYASHI, *ibid.* **96** (1988) 525.
13. K. YASUDA, S. D. KIM, Y. KANEMICHI, Y. MATSUO and S. KIMURA, *ibid.* **98** (1990) 1103.
14. K. YASUDA, S. OHSAWA, Y. MATSUO and S. KIMURA, *J. Mater. Sci. Japan* **41** (1992) 482.
15. K. YASUDA, J. TATAMI, K. ASADA, Y. MATSUO and S. KIMURA, *J. Ceram. Soc. Japan* **101** (1993) 1384.
16. K. YASUDA, J. TATAMI, Y. MATSUO and S. KIMURA, *ibid.* **102** (1994) 887.
17. W. FELLER "An introduction to probability theory", Vol 1 (John Wiley & Sons, Inc., 1970) p. 146.
18. S. N. CHATTERJEE, *Int. J. Solids & Struc.* **11** (1975) 521.
19. W. D. KINGERY, *J. Amer. Ceram. Soc.* **37** (1954) 42.

Received 19 April
and accepted 13 November 1996